

Mixing time and simulated annealing for the stochastic cellular automata

Bruno Hideki Fukushima-Kimura^{*,†}

Satoshi Handa[‡]

Katsuhiro Kamakura[§]

Yoshinori Kamijima[¶]

Kazushi Kawamura^{||}

Akira Sakai^{*,**}

June 6, 2022

Abstract

Finding a ground state of a given Hamiltonian on a graph $G = (V, E)$ is an important but hard problem. The standard approach for this kind of problem is the application of algorithms that rely on single spin-flip Markov chain Monte Carlo methods such as the simulated annealing based on Glauber or Metropolis dynamics. In this paper, we investigate a particular kind of stochastic cellular automata, in which all spins are updated independently and simultaneously. We prove that (i) if the temperature is fixed sufficiently high, then the mixing time is at most of order $\log |V|$, and that (ii) if the temperature drops in time n as $1/\log n$, then the limiting measure is uniformly distributed over the ground states.

1 Introduction and main results

There are several occasions in real life when we have to quickly choose one among extremely many options. In addition, we want our choice to be optimal in a certain sense. Such combinatorial optimization problems are ubiquitous and possibly quite hard to be solved in a fast way. In particular, polynomial-time algorithms for NP-hard problems are not known to exist [8].

One possible approach to find an optimal solution to a given problem is to translate it into an Ising Hamiltonian on a finite graph $G = (V, E)$ with no multi- or self-edges (see, e.g., [17] for a list of examples of such mappings) and find one of its ground states that corresponds to an optimal solution. Given a system of spin-spin couplings $\{J_{x,y}\}_{x,y \in V}$ (with $J_{x,y} = J_{y,x}$, and $J_{x,y} = 0$ if $\{x, y\} \notin E$) and external magnetic fields $\{h_x\}_{x \in V}$, we define the Ising Hamiltonian

^{*}Faculty of Science, Hokkaido University.

[†]Corresponding author: bruno@math.sci.hokudai.ac.jp

[‡]atama plus K.K.

[§]TOME R&D Inc.

[¶]National Center for Theoretical Sciences (NCTS).

^{||}Institute of Innovative Research, Tokyo Institute of Technology.

^{**}<https://orcid.org/0000-0003-0943-7842>

of a spin configuration $\sigma = \{\sigma_x\}_{x \in V} \in \Omega \equiv \{\pm 1\}^V$ as

$$H(\sigma) = - \sum_{\{x,y\} \in E} J_{x,y} \sigma_x \sigma_y - \sum_{x \in V} h_x \sigma_x \equiv -\frac{1}{2} \sum_{x,y \in V} J_{x,y} \sigma_x \sigma_y - \sum_{x \in V} h_x \sigma_x. \quad (1.1)$$

Let GS denote the set of ground states, the configurations at which the Hamiltonian attains its minimum value, i.e.,

$$\text{GS} = \arg \min_{\sigma} H(\sigma) \equiv \{\sigma \in \Omega : H(\sigma) = \min_{\tau} H(\tau)\}. \quad (1.2)$$

A method that can possibly be considered in the search for ground states is to use a Markov chain Monte Carlo (MCMC) to sample the Gibbs distribution $\pi_{\beta}^G \propto e^{-\beta H}$ at the inverse temperature $\beta \geq 0$:

$$\pi_{\beta}^G(\sigma) = \frac{w_{\beta}^G(\sigma)}{\sum_{\tau} w_{\beta}^G(\tau)}, \quad \text{where} \quad w_{\beta}^G(\sigma) = e^{-\beta H(\sigma)}. \quad (1.3)$$

Obviously, the Gibbs distribution attains its highest peaks on GS.

There are several MCMCs that can generate the Gibbs distribution as the equilibrium measure. One of them is the Glauber dynamics [10], which is defined by the transition probability

$$P_{\beta}^G(\sigma, \tau) = \begin{cases} \frac{1}{|V|} \frac{w_{\beta}^G(\sigma^x)}{w_{\beta}^G(\sigma) + w_{\beta}^G(\sigma^x)} & [\tau = \sigma^x], \\ 1 - \sum_{x \in V} P_{\beta}^G(\sigma, \sigma^x) & [\tau = \sigma], \\ 0 & [\text{otherwise}], \end{cases} \quad \text{where} \quad (\sigma^x)_y = \begin{cases} \sigma_y & [y \neq x], \\ -\sigma_y & [y = x]. \end{cases} \quad (1.4)$$

Notice that, by introducing the cavity fields

$$\tilde{h}_x(\sigma) = \sum_{y \in V} J_{x,y} \sigma_y + h_x, \quad (1.5)$$

the transition probability $P_{\beta}^G(\sigma, \sigma^x)$ can also be written as

$$P_{\beta}^G(\sigma, \sigma^x) = \frac{1}{|V|} \frac{e^{-\beta \tilde{h}_x(\sigma) \sigma_x}}{2 \cosh(\beta \tilde{h}_x(\sigma))}. \quad (1.6)$$

Since P_{β}^G is aperiodic, irreducible and reversible with respect to π_{β}^G , i.e., $\pi_{\beta}^G(\sigma) P_{\beta}^G(\sigma, \tau) = \pi_{\beta}^G(\tau) P_{\beta}^G(\tau, \sigma)$ holds for all $\sigma, \tau \in \Omega$, then the Gibbs distribution is the unique equilibrium distribution for the Glauber dynamics. The transition probability $P_{\beta}^G(\sigma, \sigma^x)$ can be interpreted as the probability of choosing a spin uniformly at random from V and then flipping it with probability proportional to $w_{\beta}^G(\sigma^x)$.

Another method that has been considered in several applications involves simulated annealing algorithms [14, 15]. The simplest example consists of an inhomogeneous Markov chain based on a single spin-flip dynamics (such as the Glauber and Metropolis dynamics) where the temperature drops every time a spin value is updated. If the temperature is set to decrease at an appropriate rate, it is guaranteed that such a procedure will converge to the ground states, see [11].

Note that, in the approaches described above, the number of spin-flips per update is at most one, which, in principle, may be improved by introducing parallel spin-flip dynamics. In respect of ferromagnetic spin systems, the Swendsen-Wang algorithm [21] is a cluster-flip MC, in which many spins may be flipped simultaneously, unlike in the Glauber and other single spin-flip dynamics. However, forming a cluster to be flipped yields strong dependency among spin variables. In recent studies such as in [18, 22], some algorithms that rely on parallel and independent spin-flips have shown significantly higher performance in identifying ground states compared to some of the well-known algorithms based on single spin-flip dynamics. For that reason, such kind of algorithms deserve some attention and a rigorous treatment from the mathematical point of view in order to understand their mechanisms and limitations becomes necessary. Furthermore, due to their main feature, we tend to be very tempted to employ hardware accelerators such as Graphics Processing Units (GPUs) to speed up simulations, which may be advantageous in the approach of solutions of real-time and time-constrained problems. So, we also include in Section 4 a brief analysis comparing the simulation times of the Glauber dynamics and the algorithms present in this paper when implemented in a CPU and a GPU.

In this paper, we investigate a particular class of probabilistic cellular automata, or PCA for short [5, 20]. Since the term PCA has already been long used as an abbreviation for principal component analysis in statistics, we would rather use the term stochastic cellular automata (SCA). It is defined by an extended version of the Hamiltonian with the addition of the pinning parameters $\mathbf{q} = \{q_x\}_{x \in V}$, which is

$$\begin{aligned}\tilde{H}(\boldsymbol{\sigma}, \boldsymbol{\tau}) &= -\frac{1}{2} \sum_{x,y \in V} J_{x,y} \sigma_x \tau_y - \frac{1}{2} \sum_{x \in V} h_x (\sigma_x + \tau_x) - \frac{1}{2} \sum_{x \in V} q_x \sigma_x \tau_x \\ &= -\frac{1}{2} \sum_{x \in V} (\tilde{h}_x(\boldsymbol{\sigma}) + q_x \sigma_x) \tau_x - \frac{1}{2} \sum_{x \in V} h_x \sigma_x.\end{aligned}\quad (1.7)$$

Let

$$w_{\beta, \mathbf{q}}^{\text{SCA}}(\boldsymbol{\sigma}) = \sum_{\boldsymbol{\tau}} e^{-\beta \tilde{H}(\boldsymbol{\sigma}, \boldsymbol{\tau})} \stackrel{(1.7)}{=} \prod_{x \in V} 2e^{\frac{\beta}{2} h_x \sigma_x} \cosh\left(\frac{\beta}{2} (\tilde{h}_x(\boldsymbol{\sigma}) + q_x \sigma_x)\right), \quad (1.8)$$

and define the SCA transition probability as

$$P_{\beta, \mathbf{q}}^{\text{SCA}}(\boldsymbol{\sigma}, \boldsymbol{\tau}) = \frac{e^{-\beta \tilde{H}(\boldsymbol{\sigma}, \boldsymbol{\tau})}}{w_{\beta, \mathbf{q}}^{\text{SCA}}(\boldsymbol{\sigma})} \stackrel{(1.7)}{=} \prod_{x \in V} \frac{e^{\frac{\beta}{2} (\tilde{h}_x(\boldsymbol{\sigma}) + q_x \sigma_x) \tau_x}}{2 \cosh\left(\frac{\beta}{2} (\tilde{h}_x(\boldsymbol{\sigma}) + q_x \sigma_x)\right)}. \quad (1.9)$$

Due to the rightmost expression of the product form, all spins in the system are updated independently and simultaneously. This implies that the SCA can transition from any spin configuration to another in just one step, which, in principle, may potentially result in a faster convergence to equilibrium. Since \tilde{H} is symmetric (due to the symmetry of J), i.e.,

$$\tilde{H}(\boldsymbol{\sigma}, \boldsymbol{\tau}) = \tilde{H}(\boldsymbol{\tau}, \boldsymbol{\sigma}), \quad \tilde{H}(\boldsymbol{\sigma}, \boldsymbol{\sigma}) = H(\boldsymbol{\sigma}) - \frac{1}{2} \sum_{x \in V} q_x, \quad (1.10)$$

the middle expression in (1.9) implies that $P_{\beta, \mathbf{q}}^{\text{SCA}}$ is reversible with respect to the equilibrium distribution

$$\pi_{\beta, \mathbf{q}}^{\text{SCA}}(\boldsymbol{\sigma}) = \frac{w_{\beta, \mathbf{q}}^{\text{SCA}}(\boldsymbol{\sigma})}{\sum_{\boldsymbol{\tau}} w_{\beta, \mathbf{q}}^{\text{SCA}}(\boldsymbol{\tau})}. \quad (1.11)$$

Although this is not the Gibbs distribution, and therefore we cannot naively use it to search for the ground states, the total-variation distance (cf., [1, Definition 4.1.1 & (4.1.5)])

$$\|\pi_{\beta, \mathbf{q}}^{\text{SCA}} - \pi_{\beta}^{\text{G}}\|_{\text{TV}} \equiv \frac{1}{2} \sum_{\sigma} |\pi_{\beta, \mathbf{q}}^{\text{SCA}}(\sigma) - \pi_{\beta}^{\text{G}}(\sigma)| = 1 - \sum_{\sigma} \pi_{\beta, \mathbf{q}}^{\text{SCA}}(\sigma) \wedge \pi_{\beta}^{\text{G}}(\sigma) \quad (1.12)$$

tends to zero as $\min_x q_x \uparrow \infty$. This is the positive side of the SCA with large \mathbf{q} . On the other hand, since the off-diagonal entries of the transition matrix $P_{\beta, \mathbf{q}}^{\text{SCA}}$ tends to zero as $\min_x q_x \uparrow \infty$, the SCA with large \mathbf{q} may well be much slower than expected. This is why we call \mathbf{q} the pinning parameters.

Having in mind the use of simulated annealing based on SCA aiming at determining the ground states, in Section 3 we investigate the SCA with the pinning parameters \mathbf{q} satisfying

$$q_x \geq \begin{cases} \sum_{y \in V} |J_{x,y}| - \frac{1}{2} \sum_{y \in C} |J_{x,y}| & [x \in C], \\ \frac{\lambda}{2} & [x \notin C], \end{cases} \quad (1.13)$$

where $C \subset V$ is an arbitrary set and λ is the largest eigenvalue of the matrix $[-J_{x,y}]_{V \times V}$. This is a sufficient condition for \tilde{H} to attain its minimum value on the diagonal entries, i.e.,

$$\min_{\sigma, \tau \in \Omega} \tilde{H}(\sigma, \tau) = \min_{\sigma \in \Omega} \tilde{H}(\sigma, \sigma), \quad \arg \min_{\sigma} \tilde{H}(\sigma, \sigma) \stackrel{(1.10)}{=} \text{GS}. \quad (1.14)$$

See [18] and its supplemental document for the proof of [18, (6)]. In this paper, we prove the following two statements:

- (i) If β is sufficiently small and fixed, then the time-homogeneous SCA has a mixing time at most of order $\log |V|$ (Theorem 2.2).
- (ii) If β_n increases in time n as $\propto \log n$, then the time-inhomogeneous SCA weakly converges to the uniform distribution π_{∞}^{G} over GS (Theorem 3.2).

The former implies faster mixing than conventional single spin-flip MCs, such as the Glauber dynamics (see Remark 2.3(i)). The latter refers to the applicability of the standard temperature-cooling schedule in the simulated annealing (see Remark 3.3(i)).

The two results above are proven mathematically rigorously, but may seem impractical. As mentioned earlier, the SCA is allowed to flip multiple spins in a single update, therefore, in principle, it potentially can reduce the mixing time when compared to other single spin-flip algorithms. However, to attain such a small mixing time as in (i), we have to keep the temperature very high (as comparable to the radius of convergence of the high-temperature expansion, see (2.5) below). Also, if we want to find a ground state by using an SCA-based simulated annealing algorithm, as stated in (ii), the temperature has to drop so slowly as $1/\log n$ (with a large multiplicative constant Γ , see (3.7) below), and therefore the number of steps required to come close to a ground state may well be extremely large. The problem seems to be due to the introduction of the total-variation distance. In order to make the distance $\|\mu - \nu\|_{\text{TV}}$ small, the two measures μ and ν have to be very close at every spin configuration. Moreover, since $\|\pi_{\beta, \mathbf{q}}^{\text{SCA}} - \pi_{\beta}^{\text{G}}\|_{\text{TV}}$ is not necessarily small for finite \mathbf{q} , we cannot tell anything about the excited states $\Omega \setminus \text{GS}$. In other words, we might be able to use the SCA under the condition (1.13) to find the best options in combinatorial optimization, but not the second- or third-best options. To overcome those difficulties, we will shortly discuss a potential replacement for the total-variation distance at the end of Section 3.

2 Mixing time for the SCA

In this section, we show that the mixing in the SCA is faster than in the Glauber dynamics when the temperature is sufficiently high. To do so, we first introduce some notions and notation.

For $\sigma, \tau \in \Omega$, we let $D_{\sigma, \tau}$ be the set of vertices at which σ and τ disagree:

$$D_{\sigma, \tau} = \{x \in V : \sigma_x \neq \tau_x\}. \quad (2.1)$$

For a time-homogeneous Markov chain, whose t -step distribution P^t converges to its equilibrium π , we define the mixing time as follows: given an $\varepsilon \in [0, 1]$,

$$t_{\text{mix}}(\varepsilon) = \inf \left\{ t \geq 0 : \max_{\sigma} \|P^t(\sigma, \cdot) - \pi\|_{\text{TV}} \leq \varepsilon \right\}.$$

In particular, we denote it by $t_{\text{mix}}^{\text{SCA}}(\varepsilon)$ when $P = P_{\beta, \mathbf{q}}^{\text{SCA}}$ and $\pi = \pi_{\beta, \mathbf{q}}^{\text{SCA}}$. Then we define the transportation metric ρ_{TM} between two probability measures on Ω as

$$\rho_{\text{TM}}(\mu, \nu) = \inf \left\{ \mathbf{E}_{\mu, \nu}[|D_{X, Y}|] : (X, Y) \text{ is a coupling of } \mu \text{ and } \nu \right\}, \quad (2.2)$$

where $\mathbf{E}_{\mu, \nu}$ is the expectation against the coupling measure $\mathbf{P}_{\mu, \nu}$ whose marginals are μ for X and ν for Y , respectively. By [16, Lemma 14.3], ρ_{TM} indeed satisfies the axioms of metrics, in particular the triangle inequality: $\rho_{\text{TM}}(\mu, \nu) \leq \rho_{\text{TM}}(\mu, \lambda) + \rho_{\text{TM}}(\lambda, \nu)$ holds for all probability measures μ, ν, λ on Ω .

The following is a summary of [16, Theorem 14.6 & Corollary 14.7], but stated in our context.

Proposition 2.1. *If there is an $r \in (0, 1)$ such that $\rho_{\text{TM}}(P(\sigma, \cdot), P(\tau, \cdot)) \leq r|D_{\sigma, \tau}|$ for any $\sigma, \tau \in \Omega$, then*

$$\max_{\sigma \in \Omega} \|P^t(\sigma, \cdot) - \pi\|_{\text{TV}} \leq r^t \max_{\sigma, \tau \in \Omega} |D_{\sigma, \tau}|. \quad (2.3)$$

Consequently,

$$t_{\text{mix}}(\varepsilon) \leq \left\lceil \frac{\log |V| - \log \varepsilon}{\log(1/r)} \right\rceil. \quad (2.4)$$

It is crucial to find a coupling (X, Y) in which the size of $D_{X, Y}$ is decreasing in average, as stated in the hypothesis of the above proposition. Here is the main statement on the mixing time for the SCA.

Theorem 2.2. *For any non-negative \mathbf{q} , if β is sufficiently small such that, independently of $\{h_x\}_{x \in V}$,*

$$r \equiv \max_{x \in V} \left(\tanh \frac{\beta q_x}{2} + \sum_{y \in V} \tanh \frac{\beta |J_{x, y}|}{2} \right) < 1, \quad (2.5)$$

then $\rho_{\text{TM}}(P_{\beta, \mathbf{q}}^{\text{SCA}}(\sigma, \cdot), P_{\beta, \mathbf{q}}^{\text{SCA}}(\tau, \cdot)) \leq r|D_{\sigma, \tau}|$ for all $\sigma, \tau \in \Omega$, and therefore $t_{\text{mix}}^{\text{SCA}}(\varepsilon)$ obeys (2.4).

Proof. It suffices to show $\rho_{\text{TM}}(P_{\beta, \mathbf{q}}^{\text{SCA}}(\boldsymbol{\sigma}, \cdot), P_{\beta, \mathbf{q}}^{\text{SCA}}(\boldsymbol{\tau}, \cdot)) \leq r$ for all $\boldsymbol{\sigma}, \boldsymbol{\tau} \in \Omega$ with $|D_{\boldsymbol{\sigma}, \boldsymbol{\tau}}| = 1$. If $|D_{\boldsymbol{\sigma}, \boldsymbol{\tau}}| \geq 2$, then, by the triangle inequality along any sequence $(\boldsymbol{\eta}_0, \boldsymbol{\eta}_1, \dots, \boldsymbol{\eta}_{|D_{\boldsymbol{\sigma}, \boldsymbol{\tau}}|})$ of spin configurations that satisfy $\boldsymbol{\eta}_0 = \boldsymbol{\sigma}$, $\boldsymbol{\eta}_{|D_{\boldsymbol{\sigma}, \boldsymbol{\tau}}|} = \boldsymbol{\tau}$ and $|D_{\boldsymbol{\eta}_{j-1}, \boldsymbol{\eta}_j}| = 1$ for all $j = 1, \dots, |D_{\boldsymbol{\sigma}, \boldsymbol{\tau}}|$, we have

$$\rho_{\text{TM}}\left(P_{\beta, \mathbf{q}}^{\text{SCA}}(\boldsymbol{\sigma}, \cdot), P_{\beta, \mathbf{q}}^{\text{SCA}}(\boldsymbol{\tau}, \cdot)\right) \leq \sum_{j=1}^{|D_{\boldsymbol{\sigma}, \boldsymbol{\tau}}|} \rho_{\text{TM}}\left(P_{\beta, \mathbf{q}}^{\text{SCA}}(\boldsymbol{\eta}_{j-1}, \cdot), P_{\beta, \mathbf{q}}^{\text{SCA}}(\boldsymbol{\eta}_j, \cdot)\right) \leq r|D_{\boldsymbol{\sigma}, \boldsymbol{\tau}}|. \quad (2.6)$$

Suppose that $D_{\boldsymbol{\sigma}, \boldsymbol{\tau}} = \{x\}$, i.e., $\boldsymbol{\tau} = \boldsymbol{\sigma}^x$. For any $\boldsymbol{\sigma} \in \Omega$ and $y \in V$, we let $p(\boldsymbol{\sigma}, y)$ be the conditional SCA probability of $\sigma_y \rightarrow 1$ given that the others are fixed (cf., (1.9)):

$$p(\boldsymbol{\sigma}, y) = \frac{e^{\frac{\beta}{2}(\tilde{h}_y(\boldsymbol{\sigma}) + q_y \sigma_y)}}{2 \cosh(\frac{\beta}{2}(\tilde{h}_y(\boldsymbol{\sigma}) + q_y \sigma_y))} = \frac{1 + \tanh(\frac{\beta}{2}(\tilde{h}_y(\boldsymbol{\sigma}) + q_y \sigma_y))}{2}. \quad (2.7)$$

Notice that $p(\boldsymbol{\sigma}, y) \neq p(\boldsymbol{\sigma}^x, y)$ only when $y = x$ or $y \in N_x \equiv \{v \in V : J_{x,v} \neq 0\}$. Using this as a threshold function for i.i.d. uniform random variables $\{U_y\}_{y \in V}$ on $[0, 1]$, we define the coupling (X, Y) of $P_{\beta, \mathbf{q}}^{\text{SCA}}(\boldsymbol{\sigma}, \cdot)$ and $P_{\beta, \mathbf{q}}^{\text{SCA}}(\boldsymbol{\sigma}^x, \cdot)$ as

$$X_y = \begin{cases} +1 & [U_y \leq p(\boldsymbol{\sigma}, y)], \\ -1 & [U_y > p(\boldsymbol{\sigma}, y)], \end{cases} \quad Y_y = \begin{cases} +1 & [U_y \leq p(\boldsymbol{\sigma}^x, y)], \\ -1 & [U_y > p(\boldsymbol{\sigma}^x, y)]. \end{cases} \quad (2.8)$$

Denote the measure of this coupling by $\mathbf{P}_{\boldsymbol{\sigma}, \boldsymbol{\sigma}^x}$ and its expectation by $\mathbf{E}_{\boldsymbol{\sigma}, \boldsymbol{\sigma}^x}$. Then we obtain

$$\begin{aligned} \mathbf{E}_{\boldsymbol{\sigma}, \boldsymbol{\sigma}^x}[|D_{X,Y}|] &= \mathbf{E}_{\boldsymbol{\sigma}, \boldsymbol{\sigma}^x} \left[\sum_{y \in V} \mathbb{1}_{\{X_y \neq Y_y\}} \right] = \sum_{y \in V} \mathbf{P}_{\boldsymbol{\sigma}, \boldsymbol{\sigma}^x}(X_y \neq Y_y) = \sum_{y \in V} |p(\boldsymbol{\sigma}, y) - p(\boldsymbol{\sigma}^x, y)| \\ &= |p(\boldsymbol{\sigma}, x) - p(\boldsymbol{\sigma}^x, x)| + \sum_{y \in N_x} |p(\boldsymbol{\sigma}, y) - p(\boldsymbol{\sigma}^x, y)|, \end{aligned} \quad (2.9)$$

where, by using the rightmost expression in (2.7),

$$|p(\boldsymbol{\sigma}, x) - p(\boldsymbol{\sigma}^x, x)| \leq \frac{1}{2} \left| \tanh \left(\frac{\beta \tilde{h}_x(\boldsymbol{\sigma})}{2} + \frac{\beta q_x}{2} \right) - \tanh \left(\frac{\beta \tilde{h}_x(\boldsymbol{\sigma})}{2} - \frac{\beta q_x}{2} \right) \right|, \quad (2.10)$$

and for $y \in N_x$,

$$\begin{aligned} |p(\boldsymbol{\sigma}, y) - p(\boldsymbol{\sigma}^x, y)| &\leq \frac{1}{2} \left| \tanh \left(\frac{\beta(\sum_{v \neq x} J_{v,y} \sigma_v + h_y + q_y \sigma_y)}{2} + \frac{\beta J_{x,y}}{2} \right) \right. \\ &\quad \left. - \tanh \left(\frac{\beta(\sum_{v \neq x} J_{v,y} \sigma_v + h_y + q_y \sigma_y)}{2} - \frac{\beta J_{x,y}}{2} \right) \right|. \end{aligned} \quad (2.11)$$

Since $|\tanh(a+b) - \tanh(a-b)| \leq 2 \tanh|b|$ for any a, b , we can conclude

$$\rho_{\text{TM}}\left(P_{\beta, \mathbf{q}}^{\text{SCA}}(\boldsymbol{\sigma}, \cdot), P_{\beta, \mathbf{q}}^{\text{SCA}}(\boldsymbol{\sigma}^x, \cdot)\right) \leq \mathbf{E}_{\boldsymbol{\sigma}, \boldsymbol{\sigma}^x}[|D_{X,Y}|] \leq \tanh \frac{\beta q_x}{2} + \sum_{y \in N_x} \tanh \frac{\beta |J_{x,y}|}{2} \leq r, \quad (2.12)$$

as required. \square

Remark 2.3. (i) It is known that, in a very general setting, the mixing time for the Glauber dynamics (1.4) is at least of order $|V| \log |V|$, see [13]. Therefore, Theorem 2.2 implies that the SCA reaches equilibrium way faster than the Glauber, as long as the temperature is high enough. Even though the result above does not play a role in practical applications and the SCA cannot be used to sample the Gibbs distribution, it does give us a hint that we may extract some benefit by considering multiple spin-flip algorithms to speed up simulations.

- (ii) It is of some interest investigating the average number of spin-flips per update, although it does not necessarily represent the speed of convergence to equilibrium. In [5], where q_x is set to be a common q for all x , the average number of spin-flips per update is conceptually explained to be $O(|V|e^{-\beta q})$. Here, we show an exact computation of the SCA transition probability and approximate it by a binomial expansion, from which we claim that the actual average number of spin-flips per update is much smaller than $O(|V|e^{-\beta q})$.

First, we recall equation (1.9). Notice that

$$\frac{e^{\frac{\beta}{2}(\tilde{h}_x(\boldsymbol{\sigma}) + q_x \sigma_x) \tau_x}}{2 \cosh(\frac{\beta}{2}(\tilde{h}_x(\boldsymbol{\sigma}) + q_x \sigma_x))} = \frac{e^{-\frac{\beta}{2}(\tilde{h}_x(\boldsymbol{\sigma}) \sigma_x + q_x)} \mathbb{1}_{\{x \in D_{\boldsymbol{\sigma}, \tau}\}}}{2 \cosh(\frac{\beta}{2}(\tilde{h}_x(\boldsymbol{\sigma}) + q_x \sigma_x))} + \frac{e^{\frac{\beta}{2}(\tilde{h}_x(\boldsymbol{\sigma}) \sigma_x + q_x)} \mathbb{1}_{\{x \in V \setminus D_{\boldsymbol{\sigma}, \tau}\}}}{2 \cosh(\frac{\beta}{2}(\tilde{h}_x(\boldsymbol{\sigma}) + q_x \sigma_x))}. \quad (2.13)$$

Isolating the q -dependence, we can rewrite the first term on the right-hand side as

$$\frac{e^{-\frac{\beta}{2}(\tilde{h}_x(\boldsymbol{\sigma}) \sigma_x + q_x)} \mathbb{1}_{\{x \in D_{\boldsymbol{\sigma}, \tau}\}}}{2 \cosh(\frac{\beta}{2}(\tilde{h}_x(\boldsymbol{\sigma}) + q_x \sigma_x))} = \underbrace{\frac{e^{-\frac{\beta}{2} q_x} \cosh(\frac{\beta}{2} \tilde{h}_x(\boldsymbol{\sigma}))}{\cosh(\frac{\beta}{2}(\tilde{h}_x(\boldsymbol{\sigma}) + q_x \sigma_x))}}_{\equiv \varepsilon_x(\boldsymbol{\sigma})} \underbrace{\frac{e^{-\frac{\beta}{2} \tilde{h}_x(\boldsymbol{\sigma}) \sigma_x}}{2 \cosh(\frac{\beta}{2} \tilde{h}_x(\boldsymbol{\sigma}))}}_{\equiv p_x(\boldsymbol{\sigma})} \mathbb{1}_{\{x \in D_{\boldsymbol{\sigma}, \tau}\}}, \quad (2.14)$$

and the second term as $(1 - \varepsilon_x(\boldsymbol{\sigma}) p_x(\boldsymbol{\sigma})) \mathbb{1}_{\{x \in V \setminus D_{\boldsymbol{\sigma}, \tau}\}}$. As a result, we obtain

$$P_{\beta, q}^{\text{SCA}}(\boldsymbol{\sigma}, \tau) = \prod_{x \in D_{\boldsymbol{\sigma}, \tau}} (\varepsilon_x(\boldsymbol{\sigma}) p_x(\boldsymbol{\sigma})) \prod_{y \in V \setminus D_{\boldsymbol{\sigma}, \tau}} (1 - \varepsilon_y(\boldsymbol{\sigma}) p_y(\boldsymbol{\sigma})). \quad (2.15)$$

Suppose that $\varepsilon_x(\boldsymbol{\sigma})$ is independent of x and $\boldsymbol{\sigma}$, which is of course untrue, and simply denote it by $\varepsilon = O(e^{-\beta q})$. Then we can rewrite $P_{\beta, q}^{\text{SCA}}(\boldsymbol{\sigma}, \tau)$ as

$$\begin{aligned} P_{\beta, q}^{\text{SCA}}(\boldsymbol{\sigma}, \tau) &\simeq \prod_{x \in D_{\boldsymbol{\sigma}, \tau}} (\varepsilon p_x(\boldsymbol{\sigma})) \prod_{y \in V \setminus D_{\boldsymbol{\sigma}, \tau}} ((1 - \varepsilon) + \varepsilon(1 - p_y(\boldsymbol{\sigma}))) \\ &= \prod_{x \in D_{\boldsymbol{\sigma}, \tau}} (\varepsilon p_x(\boldsymbol{\sigma})) \sum_{S: D_{\boldsymbol{\sigma}, \tau} \subset S \subset V} (1 - \varepsilon)^{|V \setminus S|} \prod_{y \in S \setminus D_{\boldsymbol{\sigma}, \tau}} (\varepsilon(1 - p_y(\boldsymbol{\sigma}))) \\ &= \sum_{S: D_{\boldsymbol{\sigma}, \tau} \subset S \subset V} \varepsilon^{|S|} (1 - \varepsilon)^{|V \setminus S|} \prod_{x \in D_{\boldsymbol{\sigma}, \tau}} p_x(\boldsymbol{\sigma}) \prod_{y \in S \setminus D_{\boldsymbol{\sigma}, \tau}} (1 - p_y(\boldsymbol{\sigma})). \end{aligned} \quad (2.16)$$

This implies that the transition from $\boldsymbol{\sigma}$ to τ can be seen as determining the binomial subset $D_{\boldsymbol{\sigma}, \tau} \subset S \subset V$ with parameter ε and then changing each spin at $x \in D_{\boldsymbol{\sigma}, \tau}$ with probability $p_x(\boldsymbol{\sigma})$. Therefore, $|V|\varepsilon$ is much larger than the actual average number of spin-flips per update.

Currently, the authors are investigating the MCMC defined by (2.16) with a constant $\varepsilon \in (0, 1]$. Some numerical results have shown better performance than the SCA in finding ground states for several problems. For more details, see Section 4.

- (iii) In fact, we can compute the average number $E^*[|D_{\sigma, X}|] \equiv \sum_{\tau} |D_{\sigma, \tau}| P^*(\sigma, \tau)$ of spin-flips per update, where X is an Ω -valued random variable whose law is $P^*(\sigma, \cdot)$. For Glauber, we have

$$E_{\beta}^G[|D_{\sigma, X}|] = \sum_{x \in V} P_{\beta}^G(\sigma, \sigma^x) = \frac{1}{|V|} \sum_{x \in V} \frac{e^{-\beta \tilde{h}_x(\sigma) \sigma_x}}{2 \cosh(\beta \tilde{h}_x(\sigma))} = \frac{1}{|V|} \sum_{x \in V} \frac{1}{e^{2\beta \tilde{h}_x(\sigma) \sigma_x} + 1}. \quad (2.17)$$

For the SCA, on the other hand, since $|D_{\sigma, \tau}| = \sum_{x \in V} \mathbb{1}_{\{\sigma_x \neq \tau_x\}}$, we have

$$\begin{aligned} E_{\beta, \mathbf{q}}^{\text{SCA}}[|D_{\sigma, X}|] &= \sum_{x \in V} \sum_{\tau: \tau_x \neq \sigma_x} P_{\beta, \mathbf{q}}^{\text{SCA}}(\sigma, \tau) = \sum_{x \in V} \frac{e^{-\frac{\beta}{2}(\tilde{h}_x(\sigma) \sigma_x + q_x)}}{2 \cosh(\frac{\beta}{2}(\tilde{h}_x(\sigma) \sigma_x + q_x))} \\ &= \sum_{x \in V} \frac{1}{e^{\beta(\tilde{h}_x(\sigma) \sigma_x + q_x)} + 1}. \end{aligned} \quad (2.18)$$

Therefore, the SCA has more spin-flips per update than Glauber, if $|V| e^{2\beta \tilde{h}_x(\sigma) \sigma_x} \geq e^{\beta(\tilde{h}_x(\sigma) \sigma_x + q_x)}$ for any $x \in V$ and $\sigma \in \Omega$, which is true when the temperature is sufficiently high such that

$$\max_{x \in V} \frac{\beta}{2} \left(q_x + |h_x| + \sum_{y \in V} |J_{x, y}| \right) \leq \log \sqrt{|V|}. \quad (2.19)$$

Compare this with the condition (2.5), which is independent of $\{h_x\}_{x \in V}$, hence better than (2.19) in this respect. On the other hand, the bound in (2.19) can be made large as $|V|$ increases, while it is always 1 in (2.5).

3 Simulated annealing for the SCA

In this section, we show that, under a logarithmic cooling schedule $\beta_t \propto \log t$, the simulated annealing for the SCA weakly converges to the uniform distribution over GS. To do so, we introduce the Dobrushin's ergodic coefficient $\delta(P)$ of the transition matrix $[P(\sigma, \tau)]_{\Omega \times \Omega}$ as

$$\delta(P) = \max_{\sigma, \tau \in \Omega} \|P(\sigma, \cdot) - P(\tau, \cdot)\|_{\text{TV}} \equiv 1 - \min_{\sigma, \eta} \sum_{\tau} P(\sigma, \tau) \wedge P(\eta, \tau). \quad (3.1)$$

The following proposition is a summary of [1, Theorems 6.8.2 & 6.8.3], but stated in our context.

Proposition 3.1. *Let $\{X_n\}_{n=0}^{\infty}$ be a time-inhomogenous Markov chain on Ω generated by the transition probabilities $\{P_n\}_{n \in \mathbb{N}}$, i.e., $P_n(\sigma, \tau) = \mathbb{P}(X_n = \tau | X_{n-1} = \sigma)$. Let $\{\pi_n\}_{n \in \mathbb{N}}$ be their respective equilibrium distributions, i.e., $\pi_n = \pi_n P_n$ for each $n \in \mathbb{N}$. If*

$$\sum_{n=1}^{\infty} \|\pi_{n+1} - \pi_n\|_{\text{TV}} < \infty, \quad (3.2)$$

and if there is a strictly increasing sequence $\{n_j\}_{j \in \mathbb{N}} \subset \mathbb{N}$ such that

$$\sum_{j=1}^{\infty} \left(1 - \delta(P_{n_j} P_{n_j+1} \cdots P_{n_{j+1}-1})\right) = \infty, \quad (3.3)$$

then there is a probability distribution π on Ω such that, for any $j \in \mathbb{N}$,

$$\lim_{n \uparrow \infty} \sup_{\mu} \|\mu P_j \cdots P_n - \pi\|_{\text{TV}} = 0, \quad (3.4)$$

where the supremum is taken over the initial distribution on Ω .

The second assumption (3.3) is a necessary and sufficient condition for the Markov chain to be weakly ergodic [1, Definition 6.8.1]: for any $j \in \mathbb{N}$,

$$\lim_{n \uparrow \infty} \sup_{\mu, \nu} \|\mu P_j \cdots P_n - \nu P_j \cdots P_n\|_{\text{TV}} = 0. \quad (3.5)$$

On the other hand, if (3.4) holds, then the Markov chain is called strongly ergodic [1, Definition 6.8.2]. The first assumption (3.2) is to guarantee strong ergodicity from weak ergodicity, as well as the existence of the limiting measure π .

To apply this proposition to the SCA, it is crucial to find a cooling schedule $\{\beta_t\}_{t \in \mathbb{N}}$ under which the two assumptions (3.2)–(3.3) hold, and to show that the limiting measure is the uniform distribution π_{∞}^{G} over GS. Here is the main statement on the simulated annealing for the SCA.

Theorem 3.2. *Suppose that the pinning parameters \mathbf{q} satisfy the condition (1.13). For any non-decreasing sequence $\{\beta_t\}_{t \in \mathbb{N}}$ satisfying $\lim_{t \uparrow \infty} \beta_t = \infty$, we have*

$$\sum_{t=1}^{\infty} \|\pi_{\beta_{t+1}, \mathbf{q}}^{\text{SCA}} - \pi_{\beta_t, \mathbf{q}}^{\text{SCA}}\|_{\text{TV}} < \infty, \quad \lim_{t \uparrow \infty} \|\pi_{\beta_t, \mathbf{q}}^{\text{SCA}} - \pi_{\infty}^{\text{G}}\|_{\text{TV}} = 0. \quad (3.6)$$

In particular, if we choose $\{\beta_t\}_{t \in \mathbb{N}}$ as

$$\beta_t = \frac{\log t}{\Gamma}, \quad \Gamma = \sum_{x \in V} \Gamma_x, \quad \Gamma_x = q_x + |h_x| + \sum_{y \in V} |J_{x,y}|, \quad (3.7)$$

then we obtain

$$\sum_{t=1}^{\infty} (1 - \delta(P_{\beta_t, \mathbf{q}}^{\text{SCA}})) = \infty. \quad (3.8)$$

As a result, for any initial $j \in \mathbb{N}$,

$$\lim_{t \rightarrow \infty} \sup_{\mu} \|\mu P_{\beta_j, \mathbf{q}}^{\text{SCA}} P_{\beta_{j+1}, \mathbf{q}}^{\text{SCA}} \cdots P_{\beta_t, \mathbf{q}}^{\text{SCA}} - \pi_{\infty}^{\text{G}}\|_{\text{TV}} = 0. \quad (3.9)$$

Proof. Since (3.9) is an immediate consequence of Proposition 3.1, (3.6) and (3.8), it remains to show (3.6) and (3.8).

To show (3.6), we first define

$$\mu_\beta(\boldsymbol{\sigma}, \boldsymbol{\tau}) = \frac{e^{-\beta \tilde{H}(\boldsymbol{\sigma}, \boldsymbol{\tau})}}{\sum_{\boldsymbol{\xi}, \boldsymbol{\eta}} e^{-\beta \tilde{H}(\boldsymbol{\xi}, \boldsymbol{\eta})}} \equiv \frac{e^{-\beta(\tilde{H}(\boldsymbol{\sigma}, \boldsymbol{\tau}) - m)}}{\sum_{\boldsymbol{\xi}, \boldsymbol{\eta}} e^{-\beta(\tilde{H}(\boldsymbol{\xi}, \boldsymbol{\eta}) - m)}}, \quad (3.10)$$

where $m = \min_{\boldsymbol{\sigma}, \boldsymbol{\eta}} \tilde{H}(\boldsymbol{\sigma}, \boldsymbol{\eta})$. Since \mathbf{q} is chosen to satisfy (1.14), we can conclude that

$$\mu_\beta(\boldsymbol{\sigma}, \boldsymbol{\tau}) = \frac{e^{-\beta(\tilde{H}(\boldsymbol{\sigma}, \boldsymbol{\tau}) - m)}}{|\text{GS}| + \sum_{\boldsymbol{\xi}, \boldsymbol{\eta}: \tilde{H}(\boldsymbol{\xi}, \boldsymbol{\eta}) > m} e^{-\beta(\tilde{H}(\boldsymbol{\xi}, \boldsymbol{\eta}) - m)}} \xrightarrow{\beta \uparrow \infty} \underbrace{\frac{\mathbb{1}_{\{\boldsymbol{\sigma} \in \text{GS}\}}}{|\text{GS}|}}_{\pi_\infty^{\text{G}}(\boldsymbol{\sigma})} \delta_{\boldsymbol{\sigma}, \boldsymbol{\tau}}. \quad (3.11)$$

Summing this over $\boldsymbol{\tau} \in \Omega \equiv \{\pm 1\}^V$ yields the second relation in (3.6). To show the first relation in (3.6), we note that

$$\frac{\partial \mu_\beta(\boldsymbol{\sigma}, \boldsymbol{\tau})}{\partial \beta} = \left(\mathbb{E}_{\mu_\beta}[\tilde{H}] - \tilde{H}(\boldsymbol{\sigma}, \boldsymbol{\tau}) \right) \mu_\beta(\boldsymbol{\sigma}, \boldsymbol{\tau}), \quad (3.12)$$

and that $\mathbb{E}_{\mu_\beta}[\tilde{H}] \equiv \sum_{\boldsymbol{\sigma}, \boldsymbol{\tau}} \tilde{H}(\boldsymbol{\sigma}, \boldsymbol{\tau}) \mu_\beta(\boldsymbol{\sigma}, \boldsymbol{\tau})$ tends to m as $\beta \uparrow \infty$, due to (3.11). Therefore, $\frac{\partial}{\partial \beta} \mu_\beta(\boldsymbol{\sigma}, \boldsymbol{\tau}) > 0$ for all β if $\tilde{H}(\boldsymbol{\sigma}, \boldsymbol{\tau}) = m$, while it is negative for sufficiently large β if $\tilde{H}(\boldsymbol{\sigma}, \boldsymbol{\tau}) > m$. Let $n \in \mathbb{N}$ be such that, as long as $\beta \geq \beta_n$, (3.12) is negative for all pairs $(\boldsymbol{\sigma}, \boldsymbol{\tau})$ satisfying $\tilde{H}(\boldsymbol{\sigma}, \boldsymbol{\tau}) > m$. As a result,

$$\begin{aligned} & \sum_{t=n}^N \|\pi_{\beta_{t+1}, \mathbf{q}}^{\text{SCA}} - \pi_{\beta_t, \mathbf{q}}^{\text{SCA}}\|_{\text{TV}} \\ &= \frac{1}{2} \sum_{\boldsymbol{\sigma} \in \text{GS}} \sum_{t=n}^N |\pi_{\beta_{t+1}, \mathbf{q}}^{\text{SCA}}(\boldsymbol{\sigma}) - \pi_{\beta_t, \mathbf{q}}^{\text{SCA}}(\boldsymbol{\sigma})| + \frac{1}{2} \sum_{\boldsymbol{\sigma} \notin \text{GS}} \sum_{t=n}^N |\pi_{\beta_{t+1}, \mathbf{q}}^{\text{SCA}}(\boldsymbol{\sigma}) - \pi_{\beta_t, \mathbf{q}}^{\text{SCA}}(\boldsymbol{\sigma})| \\ &\leq \frac{1}{2} \sum_{\boldsymbol{\sigma} \in \text{GS}} \sum_{t=n}^N (\mu_{\beta_{t+1}}(\boldsymbol{\sigma}, \boldsymbol{\sigma}) - \mu_{\beta_t}(\boldsymbol{\sigma}, \boldsymbol{\sigma})) + \frac{1}{2} \sum_{\boldsymbol{\sigma} \in \text{GS}} \sum_{\boldsymbol{\tau} \neq \boldsymbol{\sigma}} \sum_{t=n}^N (\mu_{\beta_t}(\boldsymbol{\sigma}, \boldsymbol{\tau}) - \mu_{\beta_{t+1}}(\boldsymbol{\sigma}, \boldsymbol{\tau})) \\ &\quad + \frac{1}{2} \sum_{\boldsymbol{\sigma} \notin \text{GS}} \sum_{t=n}^N (\pi_{\beta_t, \mathbf{q}}^{\text{SCA}}(\boldsymbol{\sigma}) - \pi_{\beta_{t+1}, \mathbf{q}}^{\text{SCA}}(\boldsymbol{\sigma})) \\ &= \frac{1}{2} \sum_{\boldsymbol{\sigma} \in \text{GS}} (\mu_{\beta_{N+1}}(\boldsymbol{\sigma}, \boldsymbol{\sigma}) - \mu_{\beta_n}(\boldsymbol{\sigma}, \boldsymbol{\sigma})) + \frac{1}{2} \sum_{\boldsymbol{\sigma} \in \text{GS}} \sum_{\boldsymbol{\tau} \neq \boldsymbol{\sigma}} (\mu_{\beta_n}(\boldsymbol{\sigma}, \boldsymbol{\tau}) - \mu_{\beta_{N+1}}(\boldsymbol{\sigma}, \boldsymbol{\tau})) \\ &\quad + \frac{1}{2} \sum_{\boldsymbol{\sigma} \notin \text{GS}} (\pi_{\beta_n, \mathbf{q}}^{\text{SCA}}(\boldsymbol{\sigma}) - \pi_{\beta_{N+1}, \mathbf{q}}^{\text{SCA}}(\boldsymbol{\sigma})) \\ &\leq \frac{3}{2} \end{aligned} \quad (3.13)$$

holds uniformly for $N \geq n$. This completes the proof of (3.6).

To show (3.8), we use the following bound on $P_{\beta, \mathbf{q}}^{\text{SCA}}$, which holds uniformly in $(\boldsymbol{\sigma}, \boldsymbol{\tau})$:

$$\begin{aligned} P_{\beta, \mathbf{q}}^{\text{SCA}}(\boldsymbol{\sigma}, \boldsymbol{\tau}) &\stackrel{(1.9)}{=} \prod_{x \in V} \frac{e^{\frac{\beta}{2}(\tilde{h}_x(\boldsymbol{\sigma}) + q_x \sigma_x) \tau_x}}{2 \cosh(\frac{\beta}{2}(\tilde{h}_x(\boldsymbol{\sigma}) + q_x \sigma_x))} \geq \prod_{x \in V} \frac{1}{1 + e^{\beta|\tilde{h}_x(\boldsymbol{\sigma}) + q_x \sigma_x|}} \\ &\stackrel{(3.7)}{\geq} \prod_{x \in V} \frac{e^{-\beta \Gamma_x}}{2} = \frac{e^{-\beta \Gamma}}{2^{|V|}}. \end{aligned} \quad (3.14)$$

Then, by (3.1), we obtain

$$\sum_{t=1}^{\infty} (1 - \delta(P_{\beta_t, \mathbf{q}}^{\text{SCA}})) = \sum_{t=1}^{\infty} \min_{\boldsymbol{\sigma}, \boldsymbol{\eta}} \sum_{\boldsymbol{\tau}} P_{\beta_t, \mathbf{q}}^{\text{SCA}}(\boldsymbol{\sigma}, \boldsymbol{\tau}) \wedge P_{\beta_t, \mathbf{q}}^{\text{SCA}}(\boldsymbol{\eta}, \boldsymbol{\tau}) \geq \sum_{t=1}^{\infty} e^{-\beta_t \Gamma}, \quad (3.15)$$

which diverges, as required, under the cooling schedule (3.7). This completes the proof of the theorem. \square

Remark 3.3. (i) The main message contained in the above theorem is that, in order to achieve weak convergence to the uniform distribution over the ground states, it is enough for the temperature to drop no faster than $1/\log t$ with a large multiplicative constant Γ . For logarithmic schedules, due to our approach, it is not trivial to ensure whether the value of Γ as in (3.7) is optimal for the SCA, contrasting with the Metropolis dynamics, whose optimal value can be theoretically determined, see [11].

(ii) Simulated annealing with the logarithmic cooling schedule may not be so practical in finding a ground state within a feasible amount of time. Instead, an exponential cooling schedule is often used in engineering. In [22], we have developed an annealing processor, called STATICA, based on the SCA with an exponential schedule. Experimental results have shown faster in searching for a ground state than conventional simulated annealing (based on the Glauber dynamics with an exponential schedule) and better performance in finding solutions to a max-cut problem.

The authors are investigating the use of exponential schedules. We do not expect weak convergence to the uniform distribution over the ground states. Instead, we want to evaluate the probability that the SCA with an exponential schedule reaches a spin configuration $\boldsymbol{\sigma}$ such that $H(\boldsymbol{\sigma}) - \min H$ is within a given error margin. A similar problem was considered by Catoni [2] for the Metropolis dynamics with an exponential schedule.

(iii) However, this may imply that we have not yet been able to make the most of the SCA's independent multi-spin flip rule for better cooling schedules. The use of the total-variation distance may be one of the reasons why we have to impose such tight conditions on the temperature; if two measures μ and ν on Ω are close in total variation, then $|\mu(\boldsymbol{\sigma}) - \nu(\boldsymbol{\sigma})|$ must be small at every $\boldsymbol{\sigma} \in \Omega$. We should keep in mind that the most important thing in combinatorial optimization is to know the ordering among spin configurations, and not to perfectly fit π_{β}^{G} by $\pi_{\beta, \mathbf{q}}^{\text{SCA}}$. For example, $\pi_{\beta, \mathbf{q}}^{\text{SCA}}$ does not have to be close to π_{β}^{G} in total variation, as long as we can say instead that $H(\boldsymbol{\sigma}) \leq H(\boldsymbol{\tau})$ (or equivalently $\pi_{\beta}^{\text{G}}(\boldsymbol{\sigma}) \geq \pi_{\beta}^{\text{G}}(\boldsymbol{\tau})$) whenever $\pi_{\beta, \mathbf{q}}^{\text{SCA}}(\boldsymbol{\sigma}) \geq \pi_{\beta, \mathbf{q}}^{\text{SCA}}(\boldsymbol{\tau})$ (see Figure 1).

In [12], we introduced a slightly relaxed version of this notion of closeness, which is also used in the stability analysis [6]. Given an error ratio $\varepsilon \in (0, 1)$, the SCA equilibrium measure $\pi_{\beta, \mathbf{q}}^{\text{SCA}}$ is said to be ε -close to the target Gibbs π_{β}^{G} in the sense of order-preservation if

$$\pi_{\beta, \mathbf{q}}^{\text{SCA}}(\boldsymbol{\sigma}) \geq \pi_{\beta, \mathbf{q}}^{\text{SCA}}(\boldsymbol{\tau}) \quad \Rightarrow \quad H(\boldsymbol{\sigma}) \leq H(\boldsymbol{\tau}) + \varepsilon R_H \quad \left(\Leftrightarrow \quad \pi_{\beta}^{\text{G}}(\boldsymbol{\sigma}) \geq \pi_{\beta}^{\text{G}}(\boldsymbol{\tau}) e^{-\beta \varepsilon R_H} \right), \quad (3.16)$$

where $R_H \equiv \max_{\boldsymbol{\sigma}, \boldsymbol{\tau}} |H(\boldsymbol{\sigma}) - H(\boldsymbol{\tau})|$ is the range of the Hamiltonian. By simple arithmetic [12] (with a little care needed due to the difference in the definition of \tilde{H}), we can show that $\pi_{\beta, \mathbf{q}}^{\text{SCA}}$ is ε -close to π_{β}^{G} if, for all $x \in V$,

$$q_x \geq |h_x| + \sum_y |J_{x,y}| + \frac{1}{\beta} \log \frac{2|V|(|h_x| + \sum_y |J_{x,y}|)}{\varepsilon R_H}. \quad (3.17)$$

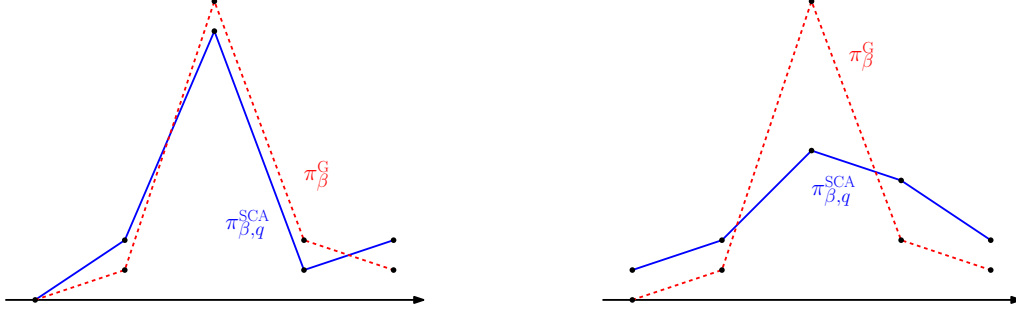


Figure 1: On the left, $\|\pi_{\beta,q}^{\text{SCA}} - \pi_{\beta}^{\text{G}}\|_{\text{TV}}$ is small, but the ordering among spin configurations is not preserved. On the right, $\|\pi_{\beta,q}^{\text{SCA}} - \pi_{\beta}^{\text{G}}\|_{\text{TV}}$ is not small, but the ordering among spin configurations is preserved.

Unfortunately, this is not better than (1.13), which we recall is a sufficient condition for $\pi_{\beta,q}^{\text{SCA}}$ to attain the highest peaks over GS, and not anywhere else. Since $|V|(|h_x| + \sum_y |J_{x,y}|)/R_H$ in the logarithmic term in (3.17) is presumably of order 1, we can say that, if the assumption (1.13) is slightly tightened to $q_x \geq |h_x| + \sum_y |J_{x,y}| + O_{\varepsilon}(\beta^{-1})$, then the SCA can be used to find not only the best options in combinatorial optimization, but also the second- and third-best options, etc. In an ongoing project, we are also aiming for improving the cooling schedule under the new notion of closeness.

4 Comparisons and simulations

Based on the discussion from Remark 2.3(ii), let us propose a new algorithm derived from the SCA studied in this paper and make a quick comparison regarding their effectiveness in obtaining the ground states. Given the inverse temperature $\beta \geq 0$ and a number $\varepsilon \in [0, 1]$, let the transition kernel of the ε -SCA be defined by

$$P_{\beta,\varepsilon}(\sigma, \tau) = \prod_{x \in D_{\sigma,\tau}} (\varepsilon p_x(\sigma)) \prod_{y \in V \setminus D_{\sigma,\tau}} (1 - \varepsilon p_y(\sigma)), \quad (4.1)$$

where we recall that

$$p_x(\sigma) = \frac{e^{-\frac{\beta}{2} \tilde{h}_x(\sigma) \sigma_x}}{2 \cosh(\frac{\beta}{2} \tilde{h}_x(\sigma))} \quad (4.2)$$

is the probability of flipping the spin σ_x from the configuration σ disregarding a pinning parameter at x . Note that $1 - \varepsilon p_x(\sigma) = (1 - \varepsilon) + \varepsilon(1 - p_x(\sigma))$. Therefore, we can visualize this new algorithm by decomposing it into two steps: in the first step the spins which are eligible to be flipped are selected independently at random, where each spin is selected with probability ε , while it remains unchanged with probability $1 - \varepsilon$; in the second step all spins which were selected in the previous step are updated simultaneously and independently, where the probability of flipping the spin at x is equal $p_x(\sigma)$.

Note that, in the particular case where $\varepsilon = 1$, the algorithm we have just introduced coincides with our SCA without the pinning parameters. Our experience has shown that, for the same Hamiltonian, cooling schedule and simulation time, the ε -SCA with appropriately

chosen parameter ε surpasses the performance of the SCA when simulated annealing is applied for obtaining ground states. We will return to the question on how the performance of this algorithm is affected by value of such parameter in the end of this section.

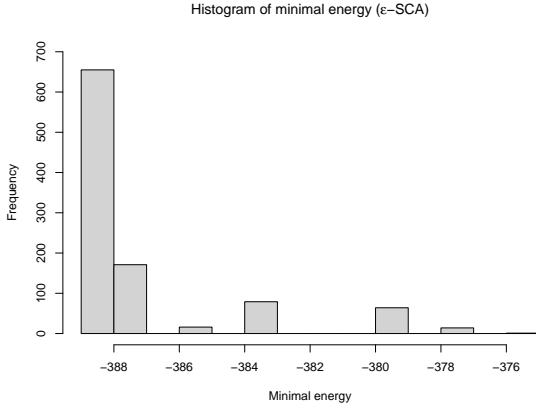
Now, let us make a comparison between the performances of the SCA (with pinning parameters taken as $q_x = \frac{\lambda}{2}$) and the ε -SCA considering the particular problems of determining the maximum cut of a given graph and the minimization of a spin-glass Hamiltonian. Even though we only have rigorous results that justify the application of logarithmic cooling schedules for the SCA, our practice also has shown that exponential cooling schedules may also work for SCA and ε -SCA, but we still do not have a solid theoretical justification for that. The plots from Figure 2 illustrate the histograms of minimal energy achieved by running 1000 trials starting from randomly chosen initial configurations considering ε -SCA and SCA, where for each trial we applied 10000 Markov chain steps and

$$\beta_t = \beta_0 \exp(\alpha t) \quad (4.3)$$

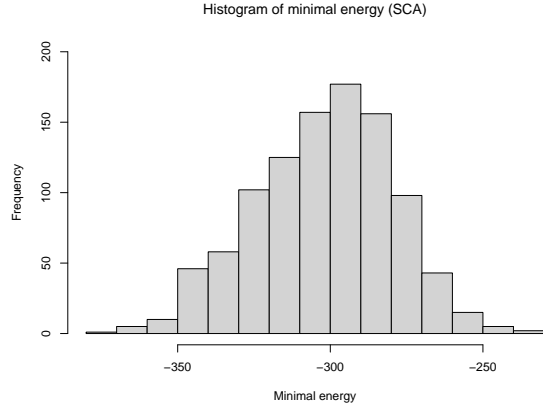
with $\beta_0 = \alpha = 10^{-3}$. First, we fixed a randomly generated Erdős–Rényi random graph $G(N, p)$ with $N = 100$ vertices and edge probability $p = 0.5$, and considered the Hamiltonian corresponding to the max-cut problem on $G(N, p)$, where $h_x = 0$ for every vertex x , and $J_{x,y} = -1$ if $\{x, y\}$ is an edge of the graph, and $J_{x,y} = 0$ otherwise. The smallest energy obtained by the ε -SCA with parameter $\varepsilon = 0.25$ was equal -389 , reached with success rate of 65.5%, while the smallest energy obtained by the SCA was -371 , reached with success rate of 0.1%, see Figures 2a and 2b. Later, we fixed a spin-glass Hamiltonian on the complete graph K_N , where $N = 100$, whose spin-spin coupling constants were taken as the realizations of mutually independent standard Gaussian random variables. In this case, we obtained the same lowest energy equal -737.2719 for both methods, however, the success rate obtained for the ε -SCA with parameter $\varepsilon = 0.8$ was 85.5%, while we obtained 27.3% for the SCA, see Figures 2c and 2d.

The role played by ε is analogous to the one played by the pinning parameters $\mathbf{q} = \{q_x\}_{x \in V}$, however, the difference is that the pinning effect for the SCA gets stronger as we decrease the temperature, so, the system will tend to flip less and less spins and might get stuck in a energetic local minimum. Regarding the ε -SCA, due to the absence of pinning parameters in the local transition probabilities and due to the effect of ε not to be influenced by the temperature, the probability of flipping a certain spin will be bigger compared to the SCA. Thus, this new algorithm allows the system to visit more configurations especially at low temperatures while preventing it from getting stuck in a local minimum. However, a rigorous explanation that indicates what leads the system to converge to a ground state is still under investigation.

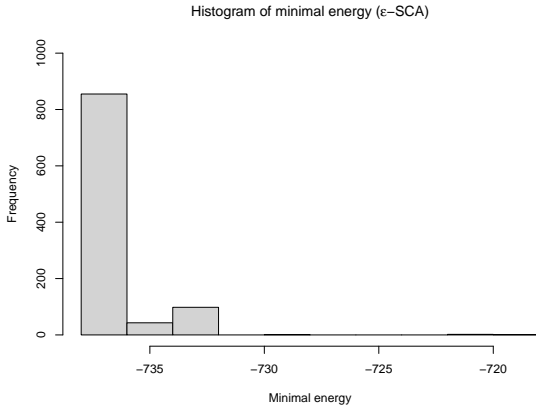
In order to get some intuition about the dependence on ε of the success rate of reaching a ground state, we considered again the same max-cut problem and spin-glass Hamiltonian, and performed 1000 ε -SCA annealing trials for different values of ε with the same cooling schedule and number of Markov chain steps as before. Typically, for Hamiltonians containing only anti-ferromagnetic spin-spin interactions (such as the Hamiltonian corresponding to the max-cut problem) such parameter ε has to be taken relatively small, since the system tends to show an oscillatory behavior and not converge to the ground states as we allow a larger number of spins to be flipped at a time, see Figure 3a. On the other hand, for the spin-glass Hamiltonian, there is a tendency of growth of the success rate as the parameter ε increases. However, when ε gets sufficiently close to 1, the algorithm behaves similarly to the SCA with pinning parameters $q_x = 0$, so, the success rate decreases since the system will not necessarily converge to a ground state of the Hamiltonian, see Figure 3b. Differently from the SCA, which we have a sufficient



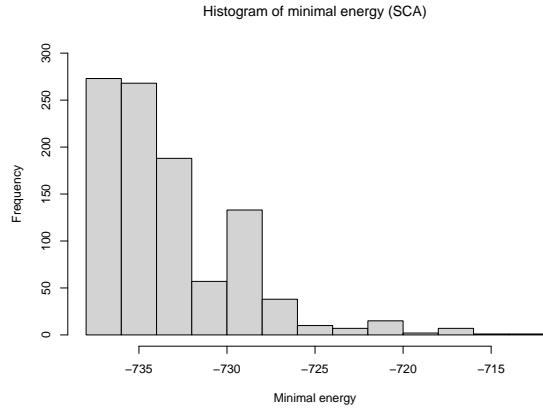
(a) Max-cut problem with ε -SCA



(b) Max-cut problem with SCA

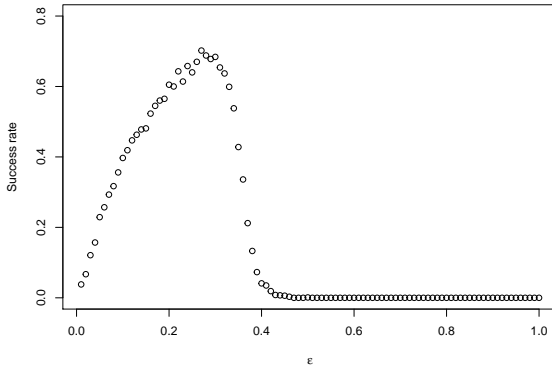


(c) Spin-glass with ε -SCA

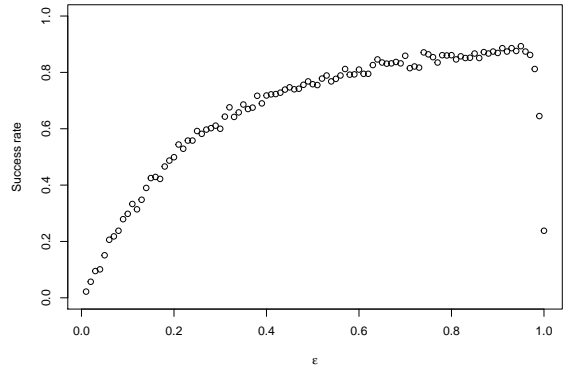


(d) Spin-glass with SCA

Figure 2: Comparison of histograms for ε -SCA and SCA.



(a) Max-cut problem



(b) Spin-glass Hamiltonian

Figure 3: Success rate of ε -SCA in obtaining a ground state as a function of the parameter ε .

Table 1: The total annealing time divided by the number of trials M (in milliseconds) corresponding to different hardware, algorithms, and number of vertices N .

M	Hardware	Algorithm	Total annealing time divided by M (in milliseconds)					
			N=128	N=256	N=512	N=1024	N=2048	N=4096
1	CPU	Glauber	0.80	0.91	1.42	2.90	8.61	27.85
1	CPU	SCA	66.01	135.03	291.36	608.94	1429.91	2868.11
1	CPU	ε -SCA	59.04	118.19	228.14	470.02	1026.73	2087.31
1	GPU	Glauber	128.92	132.61	131.58	140.54	154.54	193.63
1	GPU	SCA	171.40	181.42	196.93	248.30	787.80	2560.36
1	GPU	ε -SCA	172.88	180.30	196.16	246.79	791.45	2561.91
128	CPU	Glauber	0.73	0.94	1.46	2.97	8.67	28.34
128	CPU	SCA	64.54	133.95	289.80	609.30	1436.82	2852.50
128	CPU	ε -SCA	57.42	117.02	227.27	467.82	1035.03	2103.27
128	GPU	Glauber	1.13	1.17	1.23	1.46	1.69	2.22
128	GPU	SCA	2.42	3.23	4.74	8.48	17.56	62.57
128	GPU	ε -SCA	2.41	3.20	4.71	8.52	17.60	62.61

condition on the pinning parameters that guarantee the convergence of the algorithm, it is still necessary to derive an analogous condition on ε .

As we mentioned previously in this paper, the parallel spin update, which is the most notorious feature shared by SCA and ε -SCA, leads us to consider hardware accelerators such as GPUs as solutions that can be very decisive in solving large-scale combinatorial problems in a shorter amount of time compared to algorithms implemented on a conventional CPU. In order to support such a claim, we evaluated the annealing time of Glauber dynamics, SCA, and ε -SCA, by implementing each algorithm in C++ (for running on a CPU) and C++/CUDA (for running on a GPU). In this evaluation, we ran the C++ code on an Intel Core i7-9700 Processor and the GPU kernel on an NVIDIA GeForce RTX 2080 Ti. Let N and M be the numbers of Ising spins and annealing trials, respectively. The execution time on a CPU is approximately proportional to $N \times M$. In contrast, thanks to the parallel computing capability, the execution efficiency can be improved on a GPU by increasing both N and M . In this evaluation, we considered Ising models with $N = 2^n$ ($7 \leq n \leq 12$) and performed simulated annealing once ($M = 1$) or 128 times ($M = 128$), where each annealing consisted of executing 2.0×10^4 Markov chain steps. The Ising models considered were derived from max-cut problems on Erdős-Rényi random graphs with $p = 0.5$. In the results summarized in Table 1, each value shows the per-annealing time (i.e., total annealing time divided by M) in milliseconds.

Although the per-annealing time for Glauber dynamics tends to be smaller compared to SCA and ε -SCA even when implemented on a GPU, such an observation can be compensated by the fact that, in [7], we observed that SCA outperformed Glauber dynamics (in terms of the success rate of finding a ground state) in most scenarios, while ε -SCA significantly outperformed both these algorithms in all considered cases. Therefore, by running several trials of ε -SCA on a GPU we can still capture a ground state with a high confidence within a relatively short period of time.

The greater effectiveness of the ε -SCA in reaching lower energy configurations compared to the SCA in several observations is very intriguing due to the lack of any rigorous mathematical justification (at the moment) for that. So, it raises several questions to be answered that brings us a new direction to be explored for the development of efficient algorithms for obtaining

ground states of Ising Hamiltonians. Moreover, in future investigations, hardware-related questions should be addressed such as memory bandwidth problems and efficient implementation of parallel spin-flip algorithms on a GPU, similarly to those explored in [4].

Acknowledgements

We are grateful to the following members for continual encouragement and stimulating discussions: Masato Motomura from Tokyo Institute of Technology; Shinya Takamaeda-Yamazaki from the University of Tokyo; Hiroshi Teramoto from Kansai University; Takashi Takemoto, Takuya Okuyama, Normann Mertig and Kasho Yamamoto from Hitachi Ltd.; Masamitsu Aoki and Suguru Ishibashi from Graduate School of Mathematics at Hokkaido University; Hisayoshi Toyokawa from Kyushu University; Yuki Ueda from Hokkaido University of Education.

References

- [1] P. Brémaud. Markov Chains, *Texts in Applied Mathematics* **31**. Springer-Verlag, New York, 1999.
- [2] O. Catoni. Rough large deviation estimates for simulated annealing: application to exponential schedules. *Ann. Probab.*, **20** (1992): 1109–1146.
- [3] V. Černý. Thermodynamical approach to the traveling salesman problem: an efficient simulation algorithm. *J. Optimiz. Theory App.*, **45** (1985): 41–51.
- [4] D. Cagigas-Muñiz, F. del Diaz-Rio, J.L. Sevillano-Ramos and J.-L. Guisado-Lizar. Efficient simulation execution of cellular automata on GPU. *Simulation Modelling Practice and Theory*, **118** (2022).
- [5] P. Dai Pra, B. Scoppola and E. Scoppola. Sampling from a Gibbs measure with pair interaction by means of PCA. *J. Stat. Phys.*, **149** (2012): 722–737.
- [6] B.H. Fukushima-Kimura, A. Sakai, H. Toyokawa and Y. Ueda. Stability of energy landscape for Ising models. *Physica A: Statistical Mechanics and its Applications*, **583** (2021).
- [7] B.H. Fukushima-Kimura, Y. Kamijima, K. Kawamura and A. Sakai. Stochastic optimization via parallel dynamics: rigorous results and simulations. *Proceedings of the ISCIE International Symposium on Stochastic Systems Theory and its Applications 2022*, 2022, 65–71.
- [8] M.R. Garey and D.S. Johnson. *Computers and Intractability: A Guide to the Theory of NP-Completeness*. W.H. Freeman and Company, San Francisco (1979).
- [9] C. Giraud. *Introduction to High-Dimensional Statistics*. Chapman & Hall/CRC, Boca Raton (2015).
- [10] R.J. Glauber. Time-dependent statistics of the Ising Model. *J. Math. Phys.*, **4** (1963): 294–307.
- [11] B. Hajek. Cooling schedules for optimal annealing. *Math. Oper. Res.*, **13** (1988): 191–376.

- [12] S. Handa, K. Kamakura, Y. Kamijima and A. Sakai. Finding optimal solutions by stochastic cellular automata. Preprint. arXiv:1906.06645.
- [13] T.P. Hayes and A. Sinclair. A general lower bound for mixing of single-site dynamics on graphs. *The Annals of Applied Probability*, **17** (2007) 931–952.
- [14] S.V. Isakov, I.N. Zintchenko, T.F. Ronnow and M. Troyer. Optimised simulated annealing for Ising spin glasses. *Comput. Phys. Commun.*, **192** (2015): 265–271.
- [15] S. Kirkpatrick, C.D. Gelatt Jr. and M.P. Vecchi. Optimization by simulated annealing. *Science*, New Series, **220** (1983): 671–680.
- [16] D.A. Levin and Y. Peres. *Markov Chains and Mixing Times, second edition*. AMS, Providence, Rhode Island (2017).
- [17] A. Lucas. Ising formulations of many NP problems. *Front. Phys.*, **12** (2014): <https://doi.org/10.3389/fphy.2014.00005>.
- [18] T. Okuyama, T. Sonobe, K. Kawarabayashi, and M. Yamaoka. Binary optimization by momentum annealing. *Phys. Rev. E* **100**, 012111 (2019).
- [19] I.N. Sanov. On the probability of large deviations of random variables. *Mat. Sbornik*, **42** (1957): 11–44. English translation in *Sel. Transl. Math. Stat. Prob.*, **1** (1961): 213–244.
- [20] B. Scoppola and A. Troiani. Gaussian mean field lattice gas. *J. Stat. Phys.*, **170** (2018): 1161–1176.
- [21] R.H. Swendsen and J.-S. Wang. Nonuniversal critical dynamics in Monte Carlo simulations. *Phys. Rev. Lett.*, **58** (1987): 86–88.
- [22] K. Yamamoto, K. Kawamura, K. Ando, N. Mertig, T. Takemoto, M. Yamaoka, H. Teramoto, A. Sakai, S. Takamaeda-Yamazaki and M. Motomura. STATICA: a 512-spin 0.25M-weight annealing processor with an all-spin-updates-at-once architecture for combinatorial optimization with complete spin-spin interactions. *IEEE Journal of Solid-State Circuits* **56** (2021): 165–178.